

## TESTING AND ANALYSIS OF PHOTOVOLTAIC MODULES FOR ELECTROCHEMICAL CORROSION

**Michael Neff**

Scanning Electron Analysis Laboratories, Inc.  
Los Angeles, California, USA

**Gordon R. Mon,  
Guy Whitla, Ron Ross, Jr.**

Jet Propulsion Laboratory  
Pasadena, California, USA

### ABSTRACT

The paper describes the testing and evaluation used to characterize the mechanisms of electrochemical corrosion of photovoltaic modules - encapsulated solar cells. The accelerated exposure testing was performed on a sample matrix of cell/encapsulant combinations, and microanalytical failure analysis on selected samples was performed in order to confirm the correlation between the accelerated test data and the life prediction model. A quantitative correlation between field exposure time and exposure time in the accelerated multi-stress tests was obtained based upon the observation that equal quantities of inter-electrode charge transfer resulted in equivalent degrees of electrochemical damage.

THE ROLE OF DIELECTRIC MATERIALS in the isolation and containment of electric charge and current has been recognized as long as electricity itself (Ref. 1). For encapsulated DC circuitry, the greater the conductance of the insulating dielectric, the greater the leakage of charge from the conducting circuitry to ground. It has also been recognized that dielectric failure is often time dependent, but there are two different forms of time dependency: 1. Either a sudden decrease in the electrical resistance after a period of time, such as in the sudden current rise for rutile after hundreds of hours at room temperature at a low voltage, (Ref. 2), which is generally attributed to the onset of hole injection under the prodding of an anode fall, which in turn increases the electron injection; 2. Or the low-stress phenomena associated with chemical changes in the dielectric due to the influx of water (humidity), ion migration (diffusion), or electrode-dielectric interaction (electrochemistry), these processes often accelerated by temperature or radiation effects. It is the latter of these two types of failure

which is of concern for the life prediction of photovoltaic devices, i.e., solar cell modules.

Solar cell modules are constructed from strings of solar cells which are encapsulated into modules, modules are wired to form panels, and panels are wired to form arrays, Figure 1. Because of this construction, the encapsulant becomes the dielectric in the system. The economics of solar cell encapsulation are such that one of three polymers is used: ethylene vinyl acetate (EVA), poly vinyl butyral (PVB), and silicone rubber (RTV). These polymers bond the cell to the glass superstrate and are sometimes protected on the rear side by a substrate film such as Tedlar. The metallization systems used include Ag paste, Ti-Pd-Ag (passivated silver, or tri-metal), and Ni systems (Ni-Sn, Ni-Pb-Sn, Ni-Cu-Sn, and Ni-Pd).

Reliability research has been focussed on the achievement of 30-year module life. Reliability testing is complicated by the fact that modules have been deployed terrestrially for only 10 to 12 years, so there is no direct knowledge of failure mechanisms in the 10 to 30 year time frame. Nonetheless, many premature field failures have been reported.

The research is further hampered by the lack of a concrete definition of failure in these devices. Because zero-resistance breakdown paths do not always occur, the definition of failure remains elusive. Nonetheless, there is a time when the output of the device drops rapidly. Therefore, a suitable definition of failure must consider the condition of the device as well as the condition of the insulation.

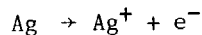
### EXPERIMENTAL

TESTING AND CHARACTERIZATION - To identify the failure mechanisms involved, a series of tests in accelerated temperature/humidity (T/H) environments were conducted initially. Many degradation phenomena were observed, including

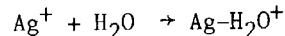
optical transmission losses in the encapsulation, Figure 2, and the dissolution and migration of metallization throughout the encapsulation, a phenomena referred to as electrochemical degradation, Figure 3. The latter phenomena was identified as a potential long term reliability problem, and a second series of refined experiments were conducted to determine the degradation rates and build a data base from which reliable life prediction capability could be established. This series of experiments were multistress tests involving exposure to accelerated levels of temperature, humidity, and voltage, where the test modules were constructed from two cells representing a cathode and an anode, Figure 4(a,b), or one cell and an aluminum bar representing the frame, Figure 5(a,b). The modules tested in these experiments were then evaluated by a number of microanalytical techniques including SEM/EDX and optical microscopy, in order to understand the degradation processes involved and to monitor the experimental method. Concurrently, these results and the results of the electrical measurements taken during the multistress tests were used to develop a model of the role of the encapsulant in the photovoltaic device electrochemical degradation, and to ultimately predict photovoltaic device service life.

**THE ELECTROCHEMICAL FAILURE MECHANISM -** Several different module degradation mechanisms were identified by optical and EDX analysis, including contamination, gas evolution, metallization delamination, and ion migration. Only the latter mechanism is addressed in this paper, i.e., the degradation resulting from electrode-dielectric interfacial interaction. A schematic representation of the mechanism is depicted in Figure 5(b). Exposure to high temperature, humidity, and voltage difference between the two electrified cells, or between an electrified cell and a grounded frame can result in dissolution of cell metallization material at the anode into the adjacent encapsulant. Driven by voltage and concentration gradients, the dissolved metallization ions diffuse through the encapsulant (wavy arrows, Fig. 5b) to the cathode where they deposit to form metallic dendrites. These dendrites "grow" back toward the anode until the encapsulant becomes insufficiently resistive to prevent the formation of a gap-bridging channel and the electrical breakdown of the insulation. The electro-chemistry and rate-limiting reactions in this process are the key elements of the degradation rate.

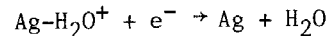
EDX analysis showed that the path of the ion migration is one of least resistance, indicated by the fact that metal ions were found preferentially on the surface of the encapsulant rather than in the encapsulant adjacent to the metallization, Figures 6 and 7. This was a very peculiar result in that it appears that the migration rate on the surface is not particularly high. A possible explanation for this phenomena is that the anode reaction



produces a positive silver ion which is quickly repelled from the anode to the surface. Once on the surface, the silver ion attaches to a polar water molecule



which continues to drift to the cathode. This heavy charged complex then migrates toward the cathode, where it dissociates and is neutralized by an electron



It is by this mechanism that ultimately the surface is connected to the cathode. A dendrite eventually grows from the cathode to the ionic silver on the surface until sufficient concentration is achieved that a conductive path is produced between the cathode and the surface above the anode. At this point, it is likely that silver ions from the anode migrate more rapidly through the encapsulant to the surface which now has become a cathode, because the electric field is increased, but even during this stage of degradation there is no short circuit because the mobility of the silver ions through the encapsulant is limited.

It was only after studying the early stages of the failure, Figure 6, and comparing the results with later stages, Figure 8, that this mechanism was understood. The microanalytical results were fundamental to the understanding.

**DEFINITION OF FAILURE -** The preceding discussion raises a question concerning the definition of a failure. It was originally thought that the dendrite growth to the surface would result in a short circuit. The view evolved from a plot of relative power output vs. interfacial charge transfer per unit length of cell edge, Figure 9, a plot derived from the multistress test results (Ref. 3). This data is practically quite significant, since it suggests that a device will fail once a given quantity of electrical charge (coulombs, C) is transferred, independent of the charge transfer mechanism.

More carefully conducted charge transfer experiments have pointed to failure mechanisms other than short circuits caused by metal bridging. One such criterion is a failure when the cell leakage current (rate of charge transfer) exceeds a pre-specified threshold value. A more relevant criterion focuses on the device rather than the dielectric, i.e., failure when sufficient metallization has dissolved off the silicon that the cell power output and its series resistance is severely compromised. Several other failures have been attributed to hydrogen evolution at the cathode which causes the encapsulant to separate from the cell, lifting the metallization with it, Figure 10. All of the results indicated that the concept of failure for these devices must

consider device performance as well as dielectric performance. Re-interpretation of the data of Figure 9 suggests that a better median cell failure criterion is 1 to 2 C/cm.

**CORRELATIONS BETWEEN TEST RESULTS AND FIELD SERVICE LIFE** - Despite the lack of a precise definition of cell electrochemical failure, a quantitative correlation between chamber test time and field service time was established. Assuming that equal amounts of charge transfer in the test and field environments result in equal amounts of degradation, it follows that (Ref. 3):

$$Y_{EQ} = \frac{Q_T}{Q_F} = \frac{V_T}{V_F} \cdot \frac{K_T \tau_T}{\sum_i K_i \tau_i} \quad (1)$$

where  $Y_{EQ}$  = years at field conditions equivalent to  $\tau_T$  hours at test conditions, yr;  $Q_T$  = total charge transferred under test conditions, C;  $Q_F$  = total yearly charge transfer under field conditions, C/yr;  $V_T$ ,  $V_F$  = test and field voltages, V;  $K_T$  = electrical conductivity of the encapsulation at the test T/H environment,  $\Omega^{-1}m^{-1}$ ;  $\tau_T$  = test time, h;  $K_i$  = electrical conductivity of the encapsulant of the field module when the cell temperature is  $T_i$  and the module internal relative humidity is  $H_i$  (Ref. 4),  $\Omega^{-1}m^{-1}$ ; and  $\tau_i$  = number of hours per year that the field module experiences a cell temperature  $T_i$  and an internal relative humidity  $H_i$ , obtained from analysis of SOLMET weather data (Ref. 3), hr/yr.

The temperature and humidity dependent PVB and EVA electrical conductivities ( $K_T$  and  $K_i$ ) were computed from formulas obtained by a global least-squares fitting of a family of polynomial equations to experimentally obtained data (Ref. 3), as plotted in Fig. 10. Clearly the insulation electrical conductivities increase as the temperature and humidity increase, indicating that these parameters are rate controlling. However, since charge transfer may be due to either electronic or ionic mobility, in the strictest sense the electrical conductivity may not be the rate limiting factor for all types of failures since many involve metallic ion charge carriers, which in turn are dependent on anion concentrations (i.e., chlorine) in the water, association rates, and dissociation rates. Nonetheless, the data appears to fit the model well, and it is evident from the microanalytical work that electronic conduction is at least partly responsible for the damage observed in all of the cases examined.

The quantities  $\sum_i K_i \tau_i$  for the several sites and encapsulants are presented in Table 1 for two scenarios: response to temperature stress only, and response to the multiple stresses of temperature and humidity. The temperature-only conditions are applicable to modules that have negligible humidity variation due to the use of moisture barriers such as metallic foils. The

temperature-plus-humidity values, on the other hand, assume instantaneous equilibrium between the partial pressure of water internal to the module at its actual operating temperature and that in the ambient.

If field and test voltages are equal, then Eq. (1) is solved for  $\tau_T$ , chamber test time equivalent to  $Y_{EQ}$  field years for the same electrode/electrolyte configuration, Figs. 11 and 12. Using these plots, chamber test conditions and test hours were determined for PVB and EVA encapsulated modules, respectively, equivalent to 30 years of field exposure at sites ranging in diversity from Miami to Boston.

At high T/H combinations, less time is required to test PVB than EVA. This results from the significantly greater sensitivity of the electrical conductivity of PVB to relative humidity. This in turn is due to the unusually large ionizable species content of that encapsulant (Ref. 6), perhaps associated with the added plasticizer, an additive lacking in EVA.

Eq. (1) can be applied to the data of Fig. 9 to ascertain equivalent field time at, say, Miami, our "worst-case" site. The data points near zero cell power output correspond to 165 yr at 500 V in Miami. The points near the knees of the curves correspond to 40 yr, and the data points just to the right and left of the short vertical line segment correspond to 4 yr at 500 V in Miami.

Eq (1) establishes an equivalence between field service time and accelerated-stress-test time based upon the concept that equal charge transfer in the two environments results in equal electrochemical damage. As such, it is useful in quantifying accelerated life testing for electrochemical solar cell degradation.

**OPTIMIZATION OF CELL CONFIGURATIONS** - A large program of electrochemical qualification tests was performed which encompassed a full matrix of cell/encapsulant configurations, results of which are reported in a separate paper (Ref. 7). Additionally, a series of experiments were conducted at 500 V in a 70°C/98% RH environment. The sample construction used in these tests was a printed Ag cell and an aluminum bar (simulating a module frame) encapsulated in PVB. One sample was tested in positive polarity (cell+, aluminum-), the other in the opposite polarity. Figs. 13 and 14 show the form of degradation after 99 test hours, equivalent to 15 years at Miami at the same voltage. Figure 13 shows the positive polarity sample exhibiting the familiar electrochemical degradation pattern of dissolved metallization, diffusion paths between anode and cathode, dendritic deposits, and entrapped bubbles evolved at the aluminum cathode. An EDX microprobe spectrum of the large dendrite, Figure 13, indicated it is primarily silver, a fact originally established by EDX analysis in the lower voltage tests, described in Ref. 3.

The negative polarity sample, Figure 14, showed none of these effects, but rather

extensive cell (cathode) surface discoloration. When the PVB was peeled away from the cell in these locations, the metallization came off the cell, indicating that the discoloration was cathodic gas evolution, probably hydrogen. The interesting aspect of the result was that the gas evolution appeared to have occurred between the metallization and the silicon.

Other pertinent data were also obtained. The insulation resistance of both samples dropped from about 1000 M to about 2.5 M. Measured unit charge transfers were 3.9 C/cm for the positive polarity sample and 3.2 C/cm for the negative polarity sample. From I-V curve data, Fig. 15, at the end of the test, power was down 30% in the positive polarity sample and 54% in the negative polarity sample, indicating that the cathode delamination (negative polarity) is more deleterious to device performance in the early stages of degradation than metal migration. More extensive tests indicated that, although the degradation mechanisms in the two polarities differed, their rates were comparable. These results are important in considering degradation in center-tapped arrays wherein modules experience both polarities of voltage stress, but at half the voltage differential to ground than would be the case for grounded single polarity arrays, indicating that center-tapped arrays would have twice the life of an otherwise identical grounded single-polarity array.

#### SUMMARY AND CONCLUSIONS

The failure analysis of degraded photovoltaic modules presented a unique challenge in sample preparation, SEM/EDX analysis, and results interpretation. The microanalytical results were fundamental to the understanding of the failure mechanisms.

Although a precise definition of device electrochemical failure is lacking, all the evidence at this time indicates that the fitted curves of Fig. 9 can be used to define a median cell-failure level per unit length of cell-frame edge.

A quantitative relationship which relates chamber test time and field service time was developed and used to predict field service life, based on the observation that equal quantities of charge transfer resulted in equal quantities of device performance degradation. This relationship is given in Eq. (1). Although not a life prediction equation, it does give the interpreter of accelerated test data a feel for what can be expected of a particular module construction in the real world, at least as pertains to terrestrial photovoltaic devices.

A significant result from the two-polarity test data is that the charge transfers for median cell failure in the two polarities are of the same order of magnitude, as are the corresponding degradation rates. This result implies that center-tapped grounded photovoltaic arrays are a preferred system configuration to

minimize electrochemical degradation, since the maximum system voltage is half that which it would otherwise be in a grounded single-polarity array.

Finally, the role of the dielectric in solar-cell electrochemical degradation has been clarified: The greater the charge carrier mobility in a particular encapsulant, the greater the cell-to-frame charge transfer, and hence the greater the electrochemical degradation.

A good dielectric from the viewpoint of photovoltaic device electrochemical degradation is one that absorbs little water, even at elevated temperature/humidity combinations, and one which exhibits a low ionic concentration and mobility in the presence of water.

Since the presence of water affects the charge carrier mobility in photovoltaic modules, further knowledge regarding the water absorption characteristics and soluble charge carrier concentrations of the transparent polymers is important in order to expand our understanding of encapsulated photovoltaic device electrochemical degradation.

**Table 1**  
The Quantity  $\sum_i K_i \tau_i$  at Selected Sites

Site	$\sum_i K_i \tau_i$ $\Omega^{-1} \text{ m}^{-1} \text{ h/yr}$			
	Temperature Acceleration		Temperature and Humidity Acceleration	
	PVB	EVA	PVB	EVA
Albuquerque	$1.12 \times 10^{-6}$	$6.27 \times 10^{-9}$	$1.89 \times 10^{-6}$	$8.78 \times 10^{-9}$
Boston	$2.96 \times 10^{-7}$	$2.24 \times 10^{-9}$	$1.26 \times 10^{-6}$	$5.11 \times 10^{-9}$
Miami	$9.11 \times 10^{-7}$	$5.88 \times 10^{-9}$	$5.72 \times 10^{-6}$	$1.66 \times 10^{-8}$

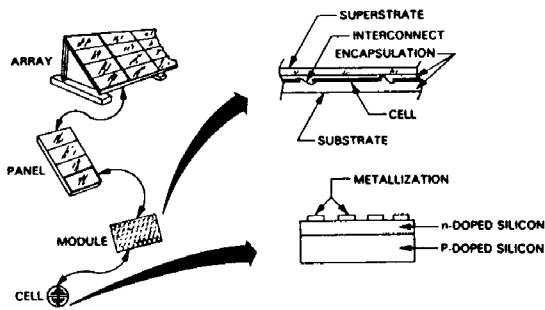


Figure 1. A schematic of photovoltaic array nomenclature.

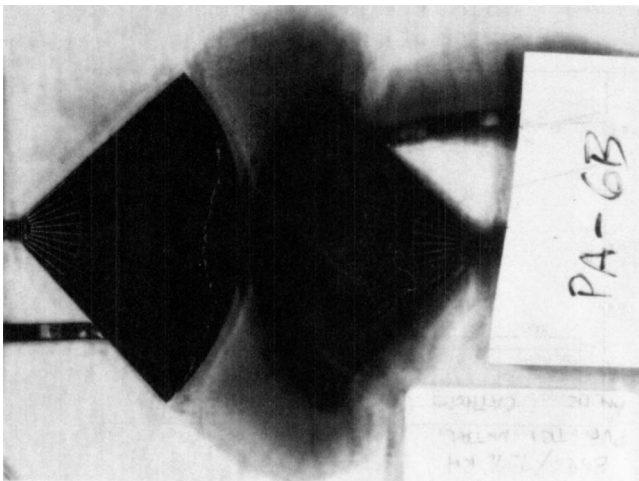


Figure 2. An optical photograph of a module failed due to optical transmission losses.

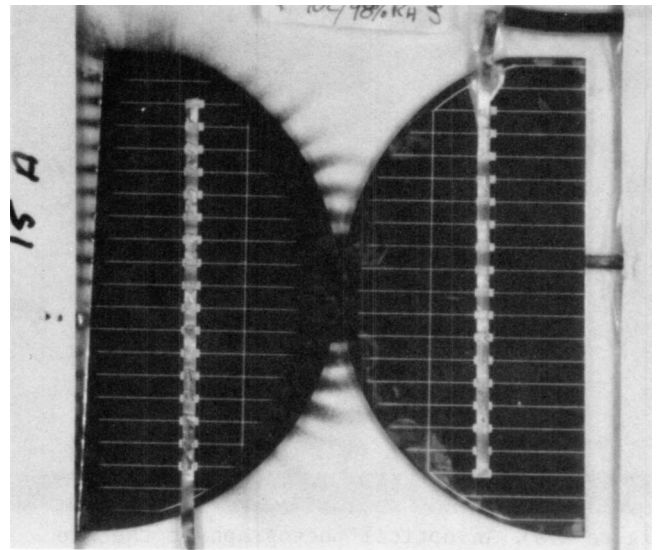


Figure 3. An optical photograph of a module failed due to metallization migration, or electrochemical degradation.

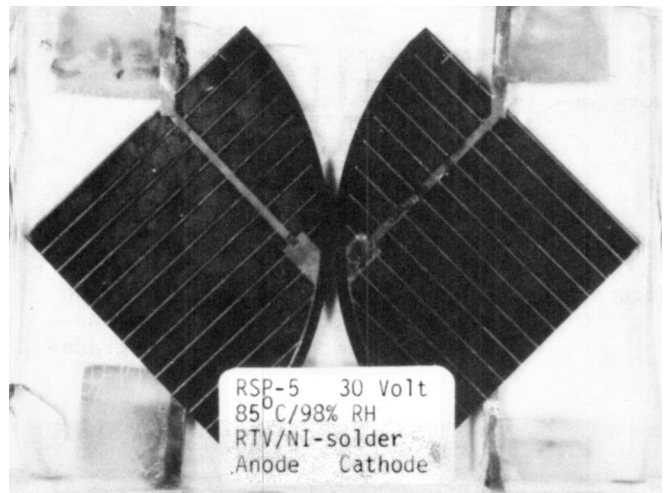


Figure 4(a). An optical photograph of the two-cell module configuration used in the multistress testing.

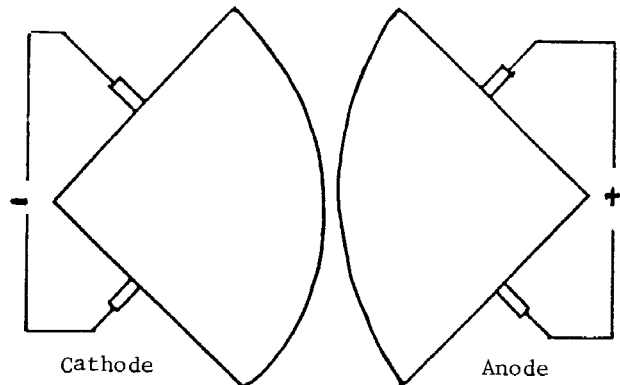


Figure 4(b). A schematic of the multistress testing configuration used.

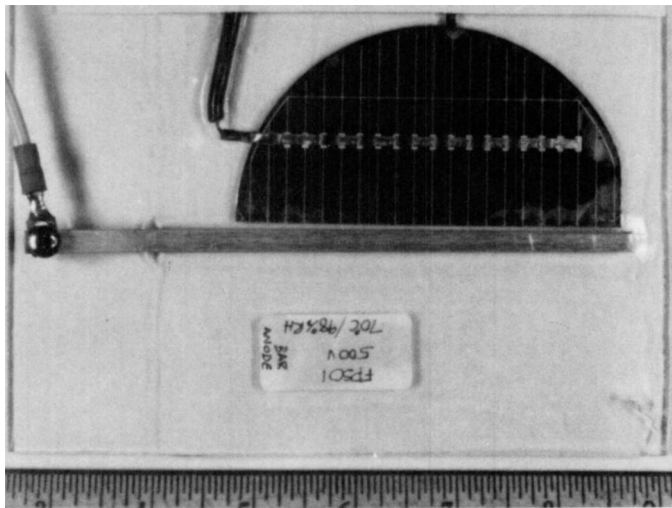


Figure 5(a). An optical photograph of the one cell-frame configuration used in multistress testing.

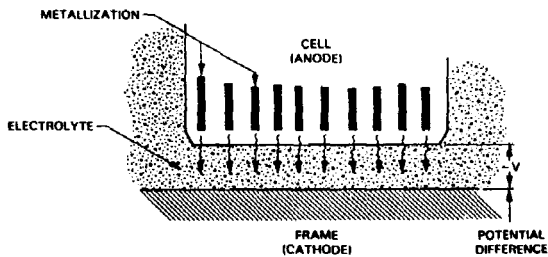


Figure 5(b). A schematic of the metallization migration mechanism, one of the forms of electrochemical degradation.

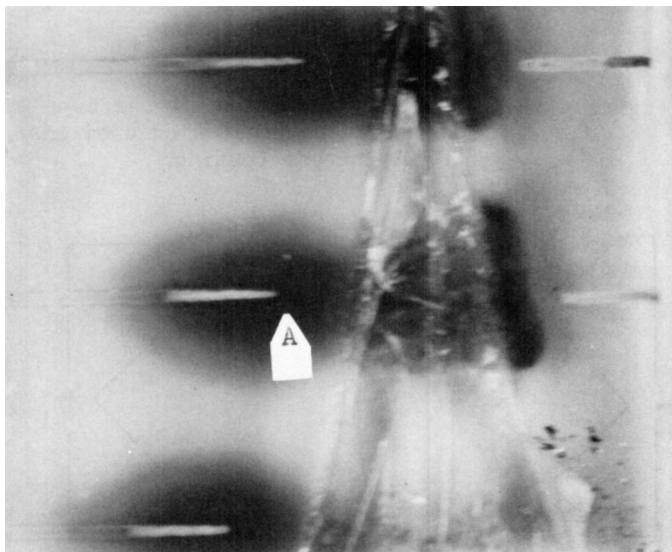


Figure 6. An optical photograph of a piece of encapsulant peeled away from the surface of a cell showing an early stage of electrochemical degradation.

```

06-MAY-84 09:58:10 EDAX READY
RATE: 1953CPS TIME 50LSEC
00-20KEY:10EV/CH PRST OFF
A:PSO-15 5674A 20R
FS= 2382 MEM: A FS= 200
|02 |04 |06 |08 |10

```

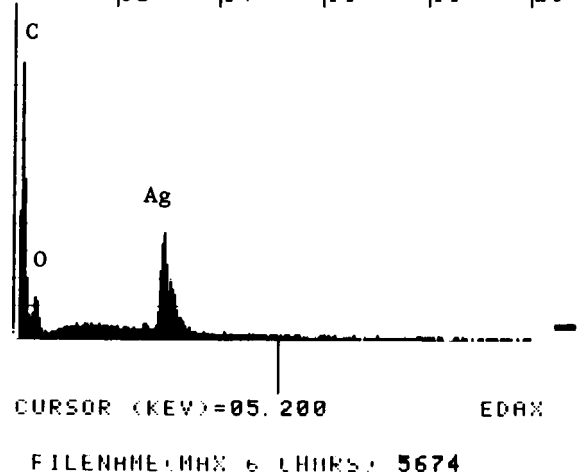


Figure 7. An EDX microprobe spectrum obtained on the top surface of the encapsulant at arrow "A", Figure 6.

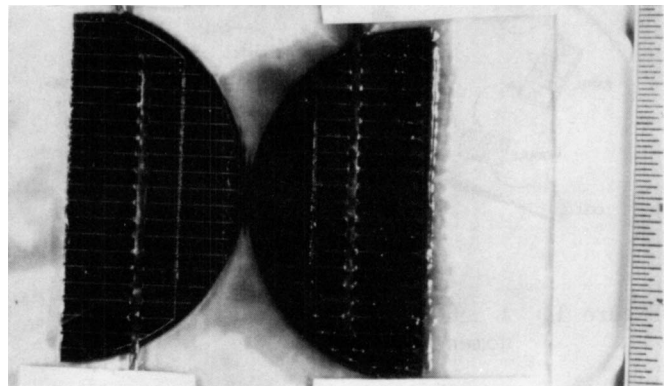


Figure 8. An optical photograph obtained on a failed module exhibiting the later stages of metal migration.

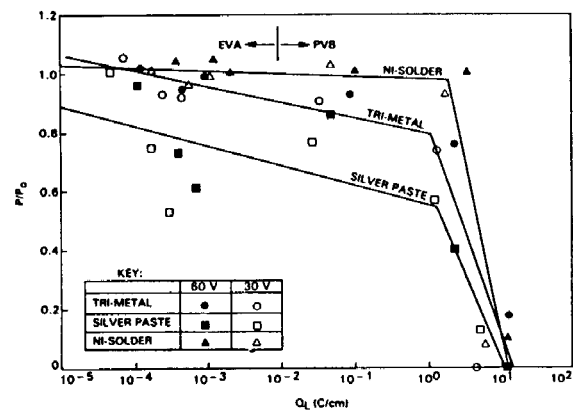


Figure 9. Normalized cell power output  $P/P_0$  versus interfacial charge transfer per unit length  $Q_L$ . (1944 hours of test exposure at 85°C and 0 to 100% relative humidity)

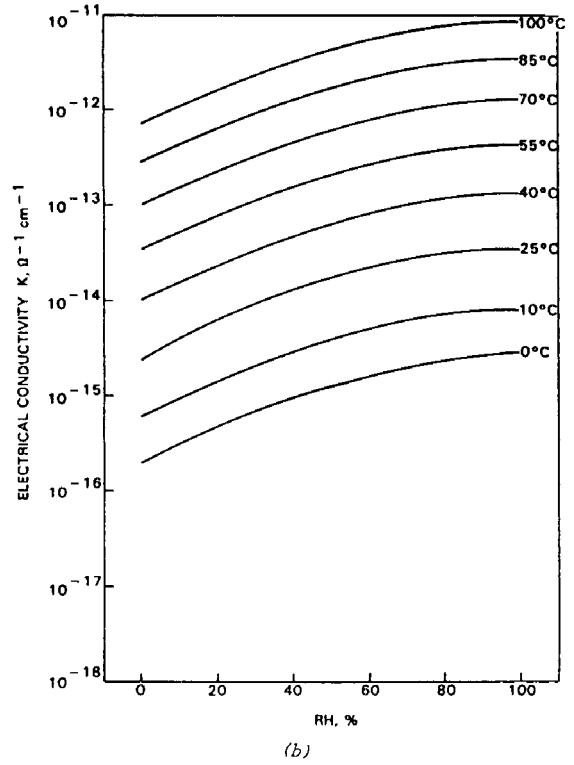
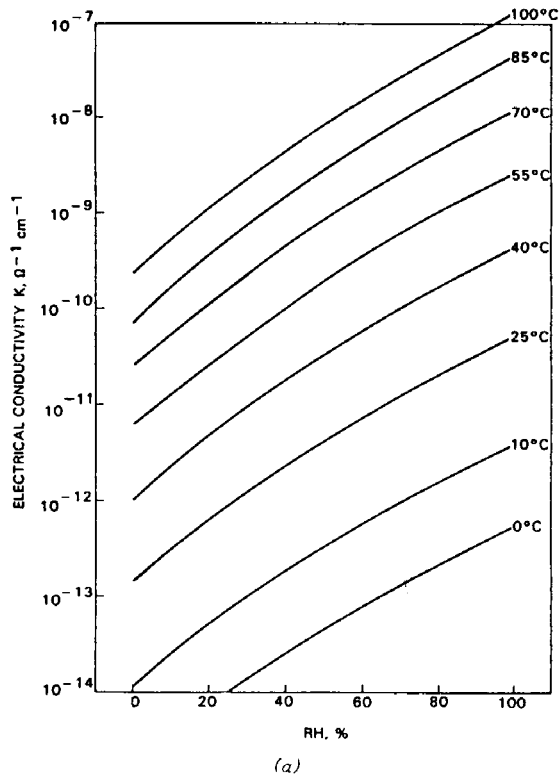


Figure 10. Electrical conductivity of PVB and EVA from 0 to 100°C relative humidity.

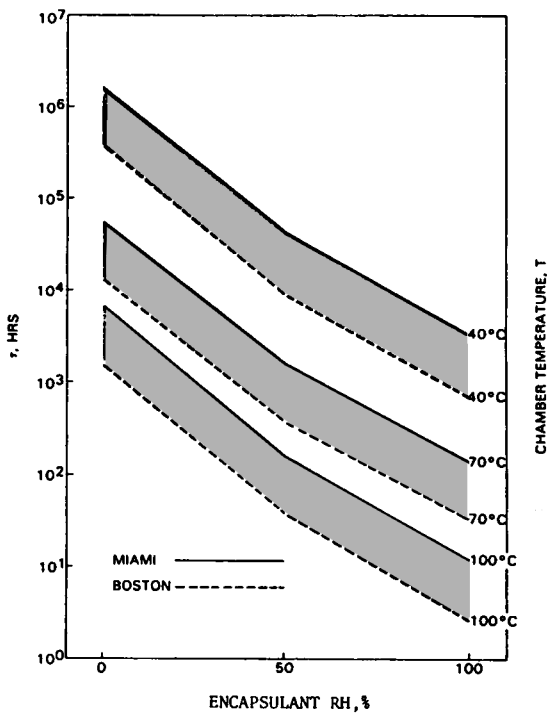


Figure 11. Test time equivalent to 30 years of field exposure for PVB-encapsulated materials.

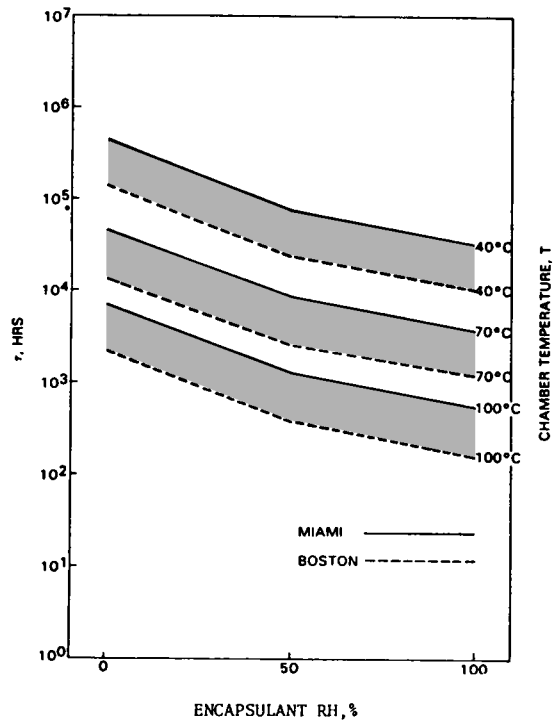


Figure 12. Test time equivalent to 30 years of field exposure for EVA-encapsulated electrodes.

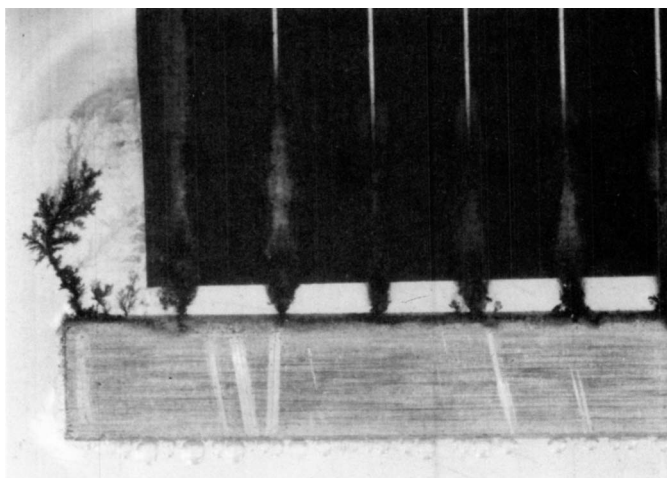


Figure 13. Positive polarity, 500 V test specimen. Cell with print Ag metallization, encapsulated in PVB. (70°C/98% relative humidity, 99 test hours).

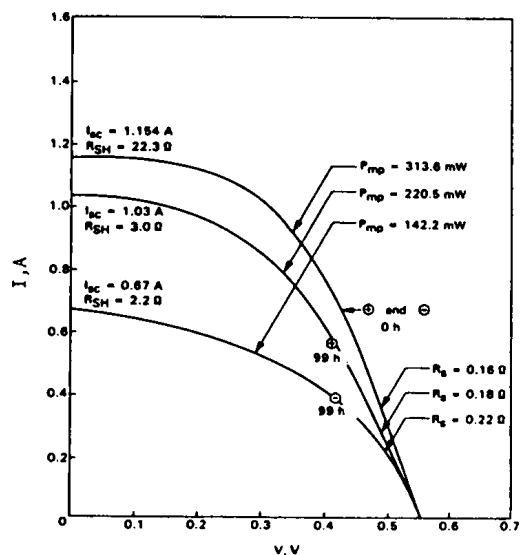


Figure 15. I-V curve data for the two-polarity experiment.

#### REFERENCES

1. J. C. Maxwell, Electricity and Magnetism, Vols. I and II, 3rd Edition, 1891, Dover Publications, Inc., 1954.
2. J. A. van Raalte, Tech. Rep. 195, Lab. Ins. Res, November, 1964.
3. G. Mon, J. Orehtsky, R. Ross, G. Whitla, "Predicting Electrochemical Breakdown in Terrestrial Photovoltaic Modules," Proceedings of the 17th IEEE Photovoltaic Specialists Conference, pp. 682-692, May 1984.
4. D. Otth and R. Ross, "Assessing Photovoltaic Module Degradation and Lifetime from Long-Term Environmental Tests," Proceedings of the 29th IES Meeting, 1983, pp. 121-126.
5. D. Otth and R. Ross, "Assessing Photovoltaic Module Life from Long-Term Environment Tests," Proceedings of the 1984 IES Conference, 1984.
6. Andre Amy, Jet Propulsion Laboratory, Personal Communications, 1983.
7. G. Mon, R. Ross, G. Whitla, and M. Neff, "The Role of Electrical Insulation in Electrochemical Degradation of Terrestrial Photovoltaic Modules," IEEE Trans. on Electrical Insulation, Vol. EI-20, December, 1985, pp. 989-996.

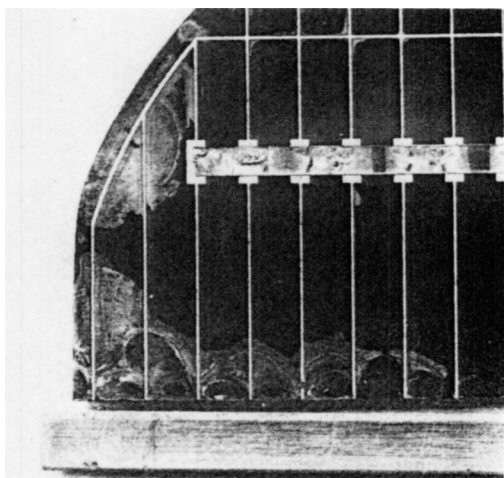


Figure 14. Negative polarity, 500 V test specimen. Cell with print Ag metallization, encapsulated in PVB. (70°C/98% relative humidity, 99 test hours).